Supplemental material

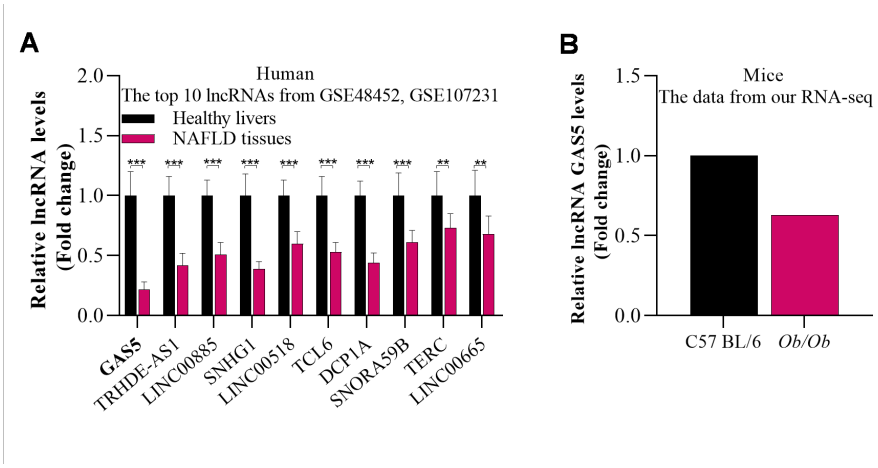

Fig. S1. GAS5 was the lncRNA with significantly changed expression identified by RNA-seq analysis of liver samples. (**A**) We first downloaded 2 human NAFLD-related microarray datasets, GSE48452 (containing 14 healthy control and 32 NAFLD tissue samples) and GSE107231 (containing 5 normal liver and 5 NAFLD biopsy tissue samples), from Gene Expression Omnibus (GEO) and analysed the downregulated lncRNAs in both datasets. Here, we reconfirmed the top 10 decreased lncRNAs by RT–qPCR in our collected clinical specimens. (**B**) GAS5 expression was also decreased in the livers of NAFLD mice as determined by lncRNA-seq analysis in our own database. The data are presented as the mean ± S.D. of three independent experiments. A p value of < 0.05 was considered statistically significant; and $^{*}p<0.05$, $^{**}p<0.01$, $^{***}p<0.001$ assessed via a two-tailed t test for examining the significance of differences between two groups; ns: not significant.

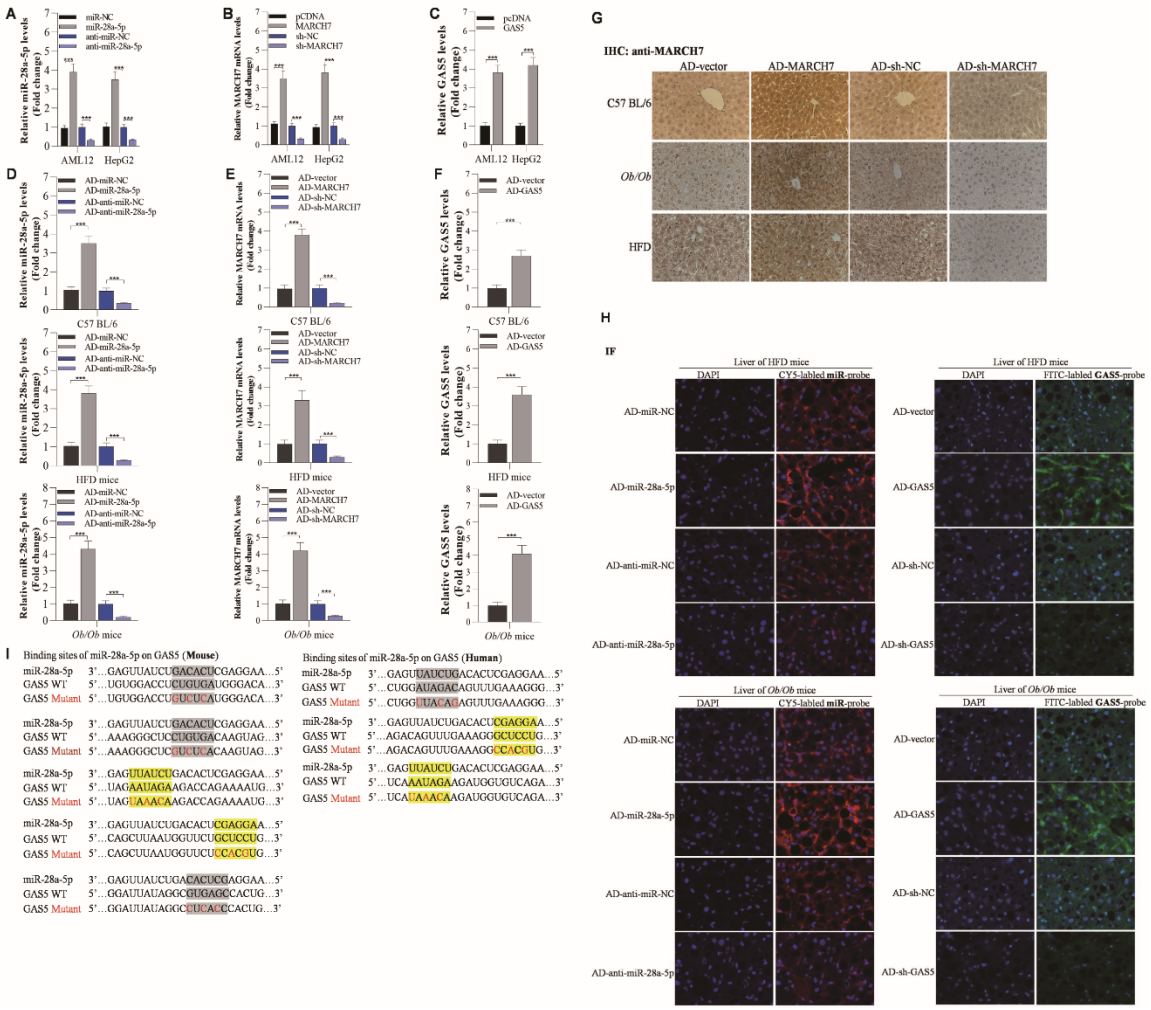

Fig. S2. The expression of siRNAs, plasmids, and adenoviruses for knockdown or overexpression of GAS5, miR-28a-5p, and MARCH7 in AML12 cells, HepG2 cells and mouse livers. In this study, AML12 and HepG2 cells were transfected with miRNAs, plasmids, or lncRNAs for 12 h. In addition, mice were injected every 10 days with adenoviruses to decrease or increase the hepatic expression of GAS5, miR-28a-5p, and MARCH7. After 3 weeks of injection, the mice were prepared for further analysis. Herein, the expression of GAS5, miR-28a-5p, and MARCH7 *in vitro* and *in vivo* was measured using RT–qPCR analysis. (**A**) The expression of miR-28a-5p in AML12 and HepG2 cells. (**B**) The expression of MARCH7 in AML12 and HepG2 cells. (**C**) GAS5 expression in AML12 and HepG2 cells. (**D**) The expression of miR-28a-5p in the livers of C57BL/6 mice, HFD-fed mice, and *Ob/Ob* mice after 3 weeks of the first injection. (**E**) The expression of MARCH7 in the livers of C57BL/6 mice, HFD-fed mice, and *Ob/Ob* mice. (**F**) The expression of GAS5 in the livers of C57BL/6 mice, HFD-fed mice, and *Ob/Ob* mice. (**G**) IHC staining of MARCH7 levels in liver of mice after 3 weeks of injection. (**H**) Immunofluorescence detecting of GAS5 and miR-28a-5p in liver of mice after 3 weeks of injection. (**I**) Additionally, the binding sites between GAS5 and miR-28a-5p were predicted by sequence alignment, and there were two conserved binding sites between GAS5 and miR-28a-5p (yellow background). The data are presented as the mean ± S.D. of three independent

experiments. Two-tailed Student's *t* test was used to determine the significance of differences between two groups (A-F). A *p* value of < 0.05 was considered statistically significant; and $^{*}p < 0.05$, $^{**}p < 0.01$, $^{***}p < 0.001$; $^{ns}p > 0.05$, ns: not significant.

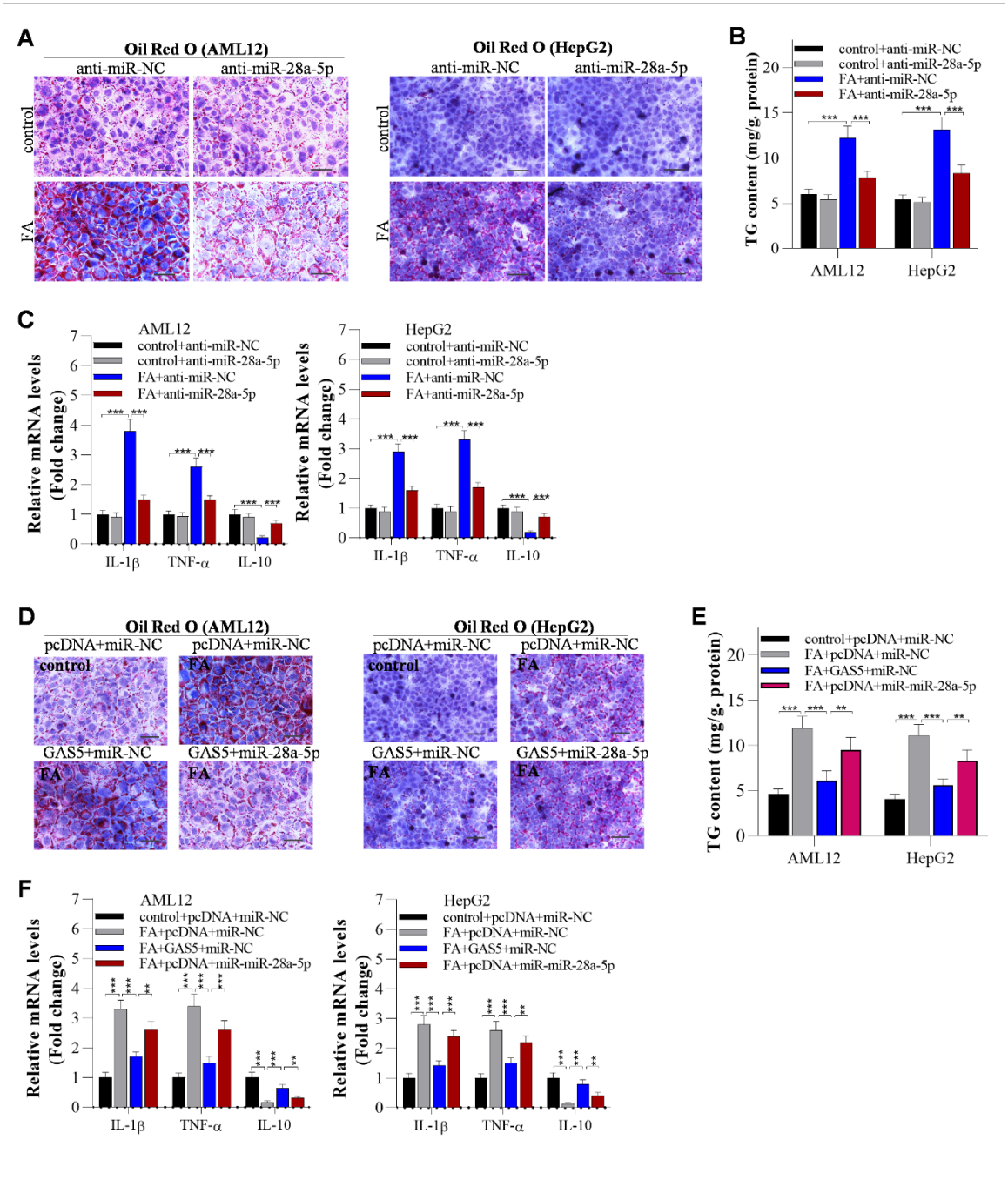

Fig. S3. miR-28a-5p knockdown inhibits lipid deposition and inflammation in AML12 and HepG2 cells (A-C). Overexpression of miR-28a-5p significantly blocks GAS5 overexpression-induced inhibition of lipid accumulation in AML12 and HepG2 cells (D-F).

On the one hand (**A-C**), AML12 and HepG2 cells were incubated with FAs for 12 h after 12 h of transfection with the indicated anti-miR-NC and anti-miR-28a-5p constructs. (**A**) Oil Red O staining; Scale bar, 50 μM. (**B**) ELISA of TG content. (**C**) RT–qPCR analysis of inflammation-related genes. On the other hand (**D-F**), we found that overexpression of miR-28a-5p blocks GAS5-controlled lipid deposition and inflammation in AML12 and HepG2 cells. (**D**) Oil Red O staining; Scale bar, 50 μM. (**E**) ELISA of TG content. (**F**) RT–qPCR analysis of inflammation-related genes. All indicated data are shown as the means ± S.D.s. A p value of < 0.05 was considered statistically significant; and $^{*}p<0.05$, $^{**}p<0.01$, $^{***}p<0.001$ assessed via a ANOVA with the Bonferroni post hoc test for comparisons among more than two groups (B, C, E, F); ns: not significant.

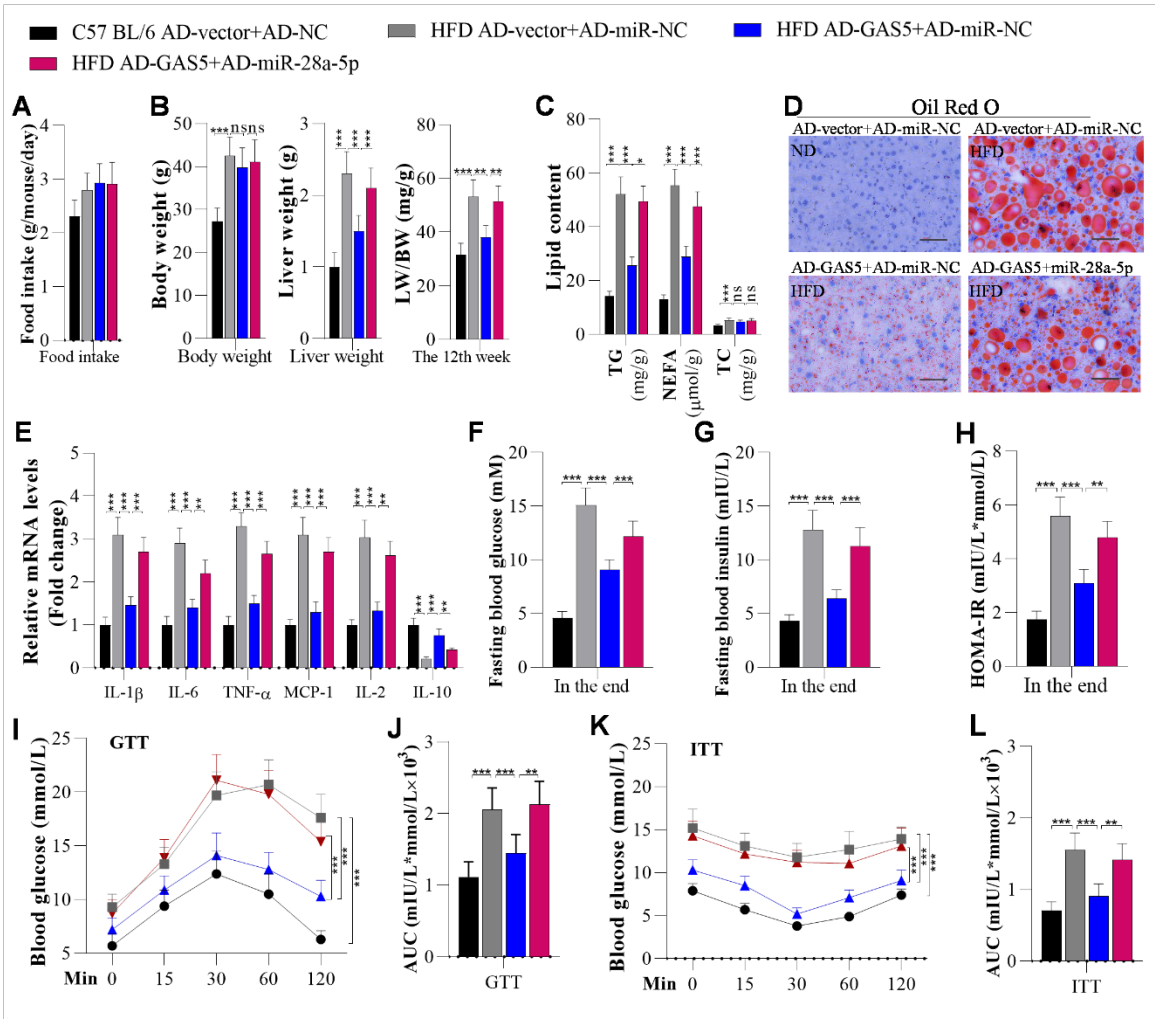

Fig. S4. Overexpression of miR-28a-5p significantly reduces GAS5 overexpression-mediated suppression of hepatic steatosis, inflammation, and insulin resistance in HFD-fed mice.

Mice were fed a ND or HFD for 12 weeks. Then, they were injected with adenoviruses every 10 days, *and* these mice were continuously fed a ND or HFD. After 3 weeks of the first injection, the mice were used for further analysis. (**A**) Food intake was measured every day during ND or HFD feeding (n=5/group). (**B**) The

body weight, liver weight, and LW/BW ratios of C57BL/6 and HFD-fed mice after 3 weeks of injection of adenoviruses (n=5/group). (**C**) TG, NEFA, and TC levels were measured using ELISA in the livers of C57BL/6 and HFD-fed mice (n=5/group). (**D**) Oil Red O staining of liver sections from adenovirus-injected C57BL/6 and HFD-fed mice (n=5/group); Scale bar, 50 μM. (**E**) The mRNA levels of inflammation-related genes analysed by RT–qPCR (n=5/group). (**F**) Fasting blood glucose levels of C57BL/6 and HFD-fed mice (n=5/group). (**G**, **H**) Fasting insulin levels and HOMA-IR scores of adenovirus-injected C57BL/6 and HFD-fed mice (n=5/group). (**I-L**) GTT and ITT of C57BL/6 and HFD-fed mice after 3 weeks of the first adenovirus injection and the areas under the curve (AUCs) for the GTT and ITT (N=5/group). The data are presented as the mean ± S.D. of three independent experiments. A p value of < 0.05 was considered statistically significant; and $^{*}p<0.05$, $^{**}p<0.01$, $^{***}p<0.001$ assessed via a ANOVA with the Bonferroni post hoc test for comparisons among more than two groups (A-L); ns: not significant.

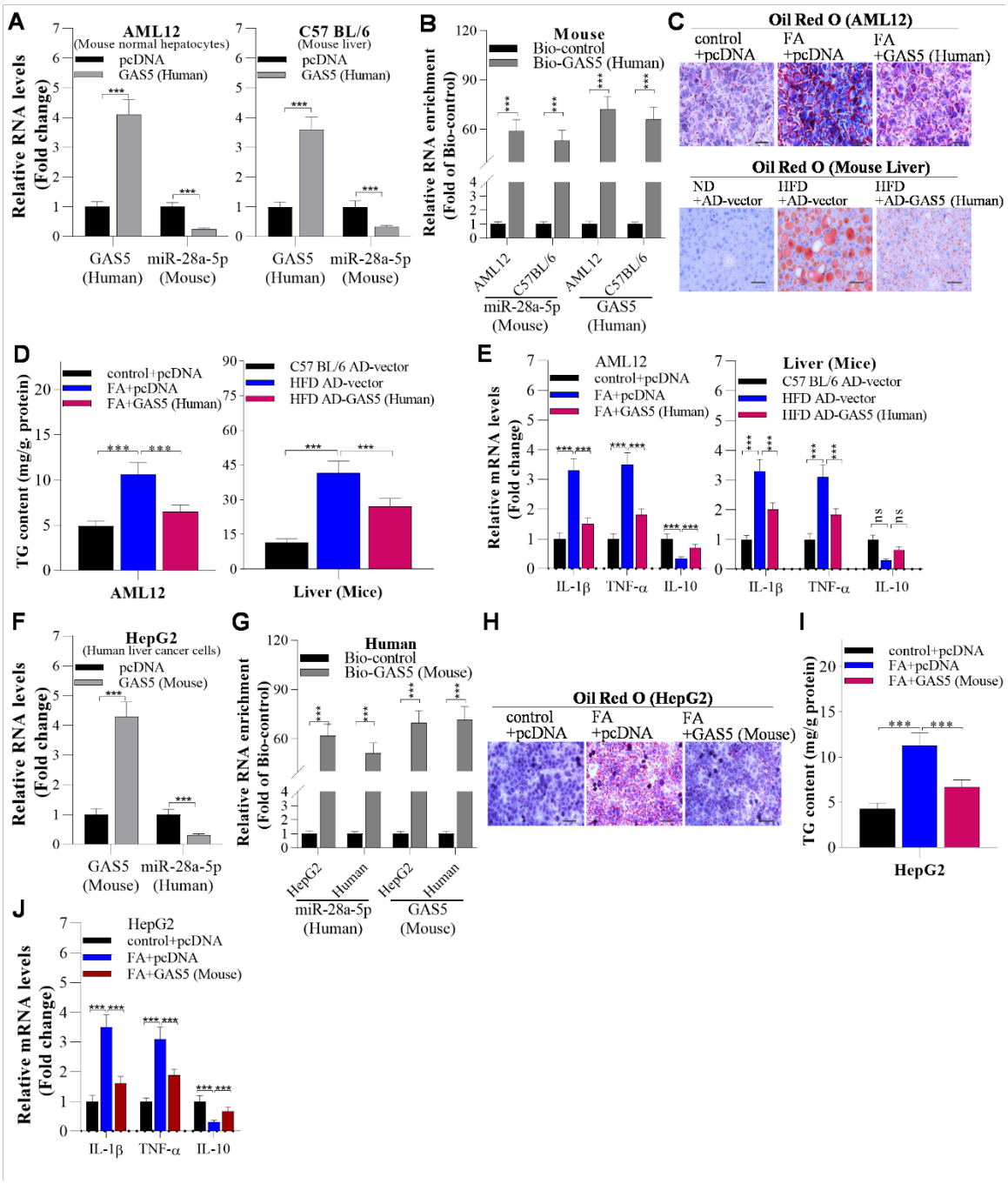

Fig. S5. Heterologous overexpression of GAS5 significantly suppresses lipid deposition and inflammation in AML12 and HepG2 cells. Because there are two conserved binding sites between GAS5/miR-28a-5p between humans and mice, we hypothesized that the functions of the GAS5/miR-28a-5p axis were also conserved in the liver between these two species. (**A**) After overexpression of human GAS5 in AML12 normal mouse hepatocytes for 12 h and in the livers of mice for one week, we examined the miR-28a-5p levels. (**B**) the Biotinylated GAS5 pull-down assay showed that human GAS5 interacted with mouse miR-28a-5p in AML12 cells and mouse liver tissues. (**C**, **D**, **E**) After overexpression of human GAS5 in AML12 cells treated with FAs for 24 h and the livers of C57BL/6 mice, we examined the lipid content and

inflammation; Scale bar, 50 μM. (**F**) After overexpression of mouse GAS5 in HepG2 human liver cancer cells for 12 hours, we determined the miR-28a-5p levels. (**G**) After overexpression of mouse GAS5 in human liver cancer HepG2 cells, we confirmed that mouse GAS5 bound to human miR-28a-5p in HepG2 cells. (**H**, **I**, **J**) After overexpression of mouse GAS5 inhibited lipid accumulation and inflammation in HepG2 cells, we evaluated the lipid content and inflammation; Scale bar, 50 μM. The data are presented as the mean ± S.D. of three independent experiments. A p value of < 0.05 was considered statistically significant; and $^{*}p<0.05$, $^{**}p<0.01$, $^{***}p<0.001$ assessed via a two-tailed t test for examining the significance of differences between two groups (A, B, F, G) or ANOVA with the Bonferroni post hoc test for comparisons among more than two groups (D, E, I, J); ns: not significant.

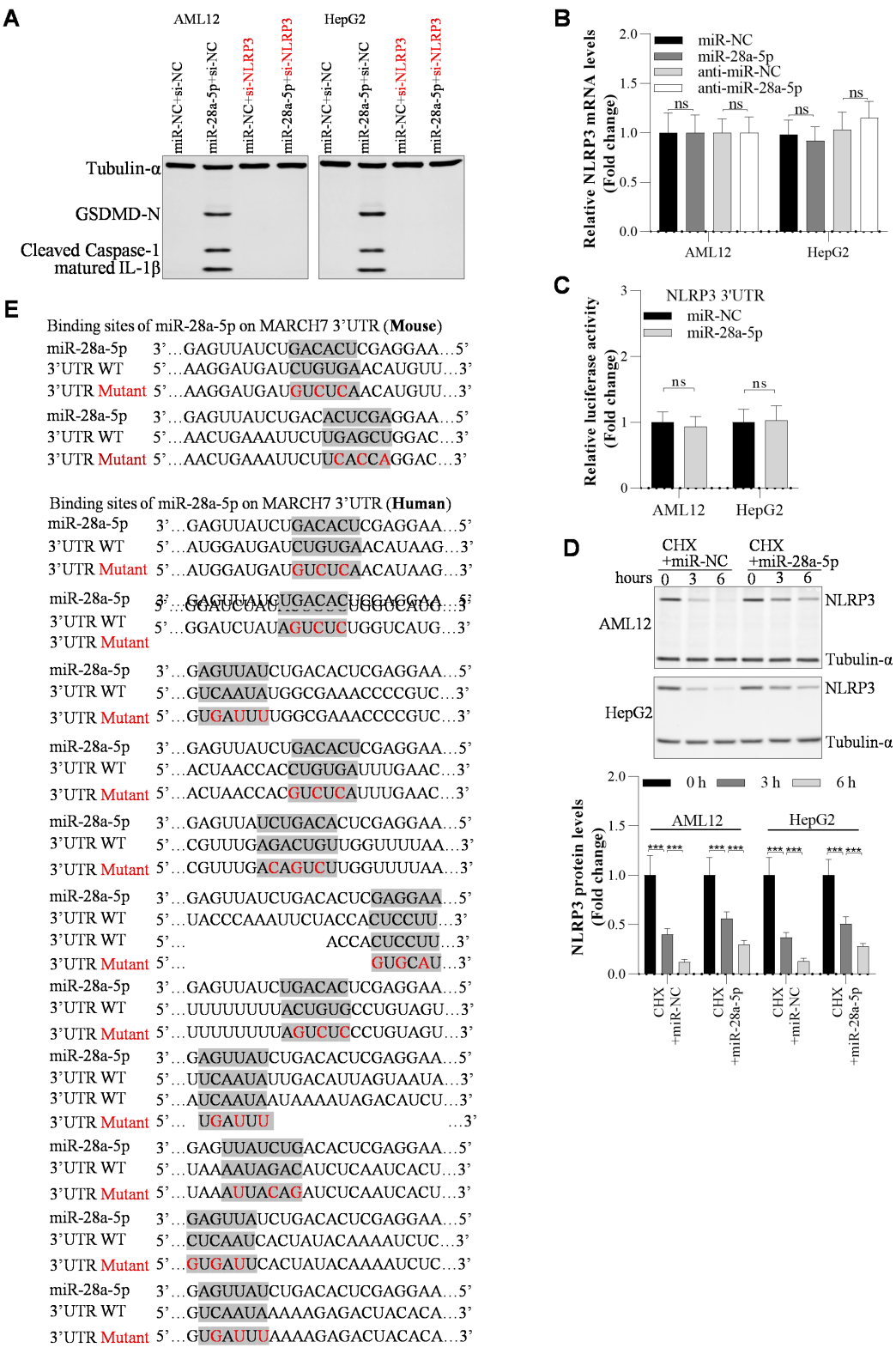

Fig. S6. Interfering with NLRP3 expression blocks miR-28a-5p-mediated activation of pyroptosis. (**A**) Interfering with NLRP3 expression blocks miR-28a-5p-mediated activation of pyroptosis, as evidenced by Western blot analysis of pyroptosis-associated proteins after 24 h of FA treatment in anti-miR-NC-, si-NC,

anti-miR-28a-5p, or si-NLRP3-transfected AML12 and HepG2 cells. (**B**) The hepatocytes were transfected with miR-NC, miR-28a-5p, anti-miR-NC, anti-miR-28a-5p for 24 h, and they were collected to determine NLRP3 mRNA expressions evidenced by RT-qPCR. (**C**) The hepatocytes were transfected with miR-NC, miR-28a-5p, and co-transfected with NLRP3 3'UTR for 24 h. Then, they were prepared for luciferase reporter assay. (**D**) miR-28a-5p significantly inhibited CHX-induced degradation of NLRP3 protein. They were incubated with 30 μM CHX along with miR-NC or miR-28a-5p transfection for 0 h, 3 h, 6 h. (**E**) The potential binding sites of miR-28a-5p in the MARCH7 3'UTR (mouse or human) were examined by sequence alignment. The data are presented as the mean ± S.D. of three independent experiments. A p value of < 0.05 was considered statistically significant; and $^{*}p<0.05$, $^{**}p<0.01$, $^{***}p<0.001$ assessed via a two-tailed t test for examining the significance of differences between two groups (B, C) or ANOVA with the Bonferroni post hoc test for comparisons among more than two groups (D); ns: not significant.

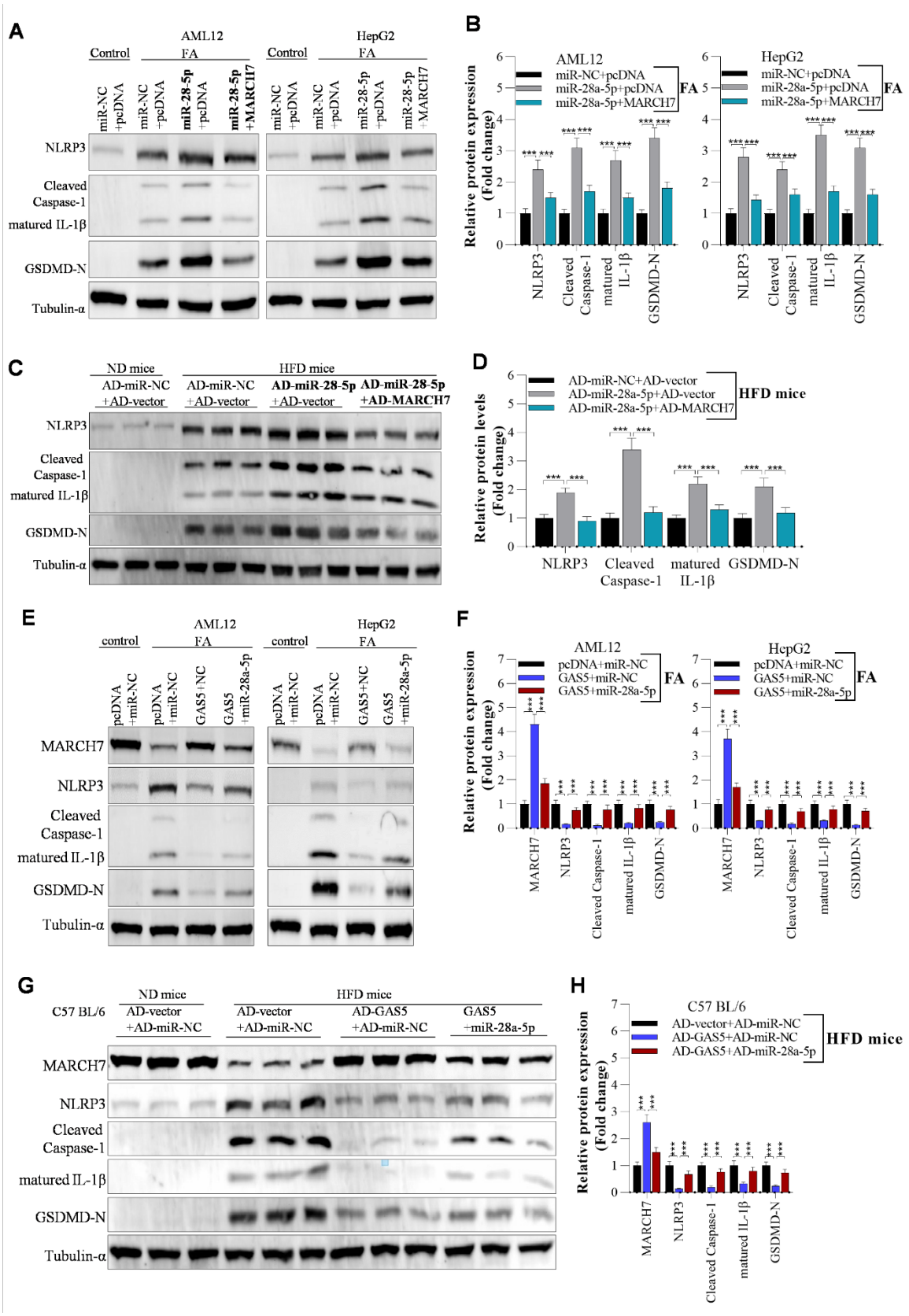

Fig. S7. MARCH7 overexpression reversed the miR-28a-5p overexpression-induced enhancement of

pyroptosis. First, AML12 and HepG2 cells were transfected with overexpression plasmids for 12 h. Then, the cells were incubated with FAs for 12 h. The cells were collected for further analysis. (**A, B**) Western blot analysis of the expression of pyroptosis-related molecules in AML12 and HepG2 cells after 24 h of transfection with miR-NC, pcDNA, miR-28a-5p, or pcDNA-MARCH7. (**C, D**) Western blot analysis of the expression of pyroptosis-related molecules in the livers of C57BL/6 mice after adenovirus injection for 7 days. All the data are shown as the means ± S.D.s. The data are presented as the mean ± S.D. of three independent experiments. (**E, F**) Western blot analysis of pyroptosis-related gene expression in AML12 and HepG2 cells after 24 h transfection with pcDNA, miR-NC, GAS5, and another 12 h of FA treatment. (**G, H**) Western blot analysis of pyroptosis-related gene expression in the livers of HFD-fed mice after 7 days of injection with adenoviruses. The data are presented as the mean ± S.D. of three independent experiments. A p value of < 0.05 was considered statistically significant; and $^{*}p<0.05$, $^{**}p<0.01$, $^{***}p<0.001$ assessed via a ANOVA with the Bonferroni post hoc test for comparisons among more than two groups (B, D, F, H); ns: not significant.

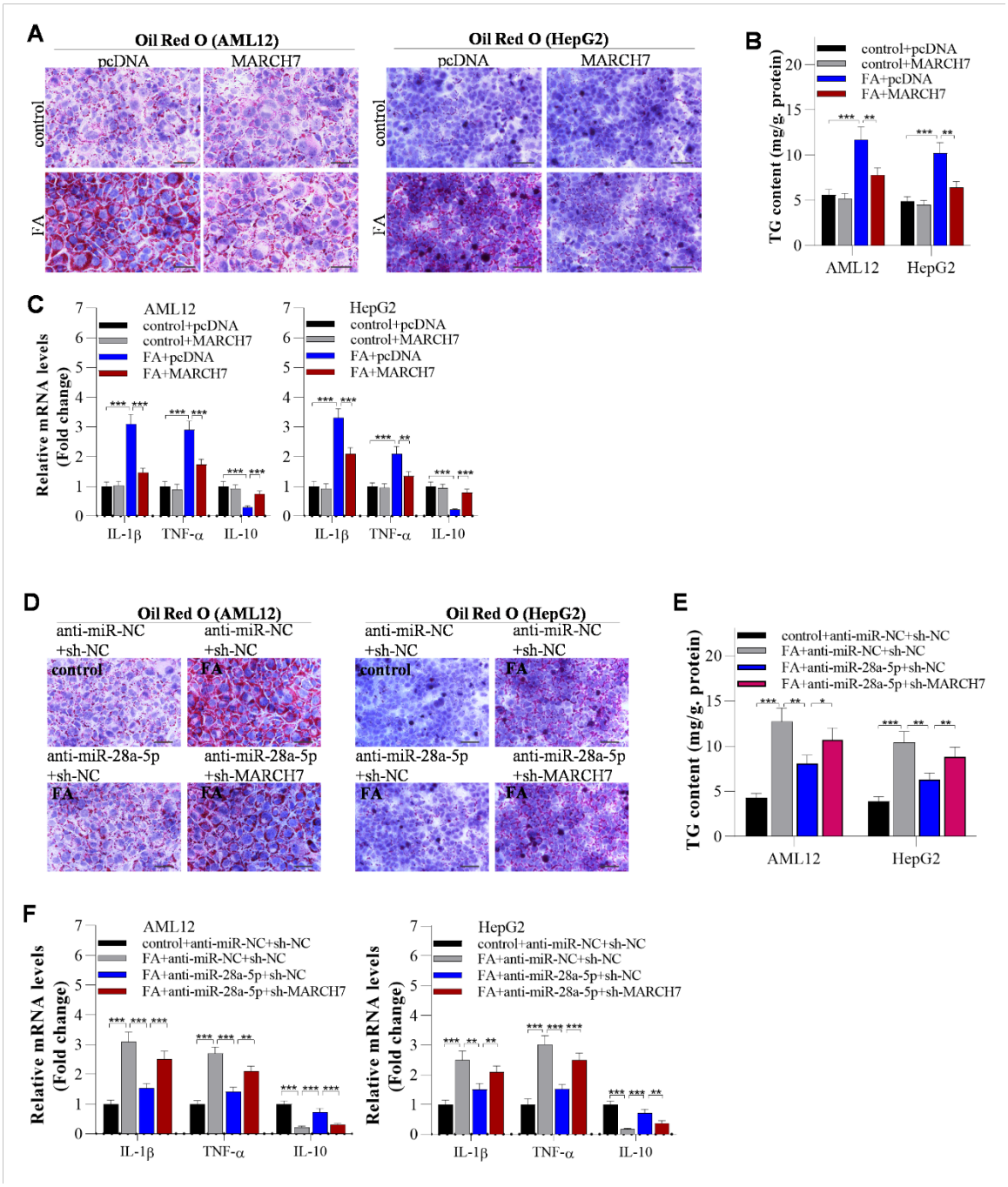

Fig. S8. Overexpression of MARCH7 attenuates lipid deposition in hepatocytes. AML12 and HepG2 cells were transfected with the indicated plasmids and miRNAs for 12 h and incubated with FAs for another 12 h. First, (**A, D**) Oil Red O staining of lipid droplets in hepatocytes; Scale bar, 50 μM. (**B, E**) ELISA of TG content in AML12 and HepG2 cells. (**C, F**) RT–qPCR assay of inflammation-related gene expression. Afterwards, we found that MARCH7 overexpression significantly inhibited FA-induced hepatic lipid accumulation and that interfering with MARCH7 expression reversed the miR-28a-5p-mediated suppression of pyroptosis in AML12 and HepG2 cells. The data are presented as the mean ± S.D. of three independent experiments. A p value of < 0.05 was considered statistically significant; and $^{*}p<0.05$, $^{**}p<0.01$, $^{***}p<0.001$

assessed via a ANOVA with the Bonferroni post hoc test for comparisons among more than two groups (B, C, E, F); ns: not significant.

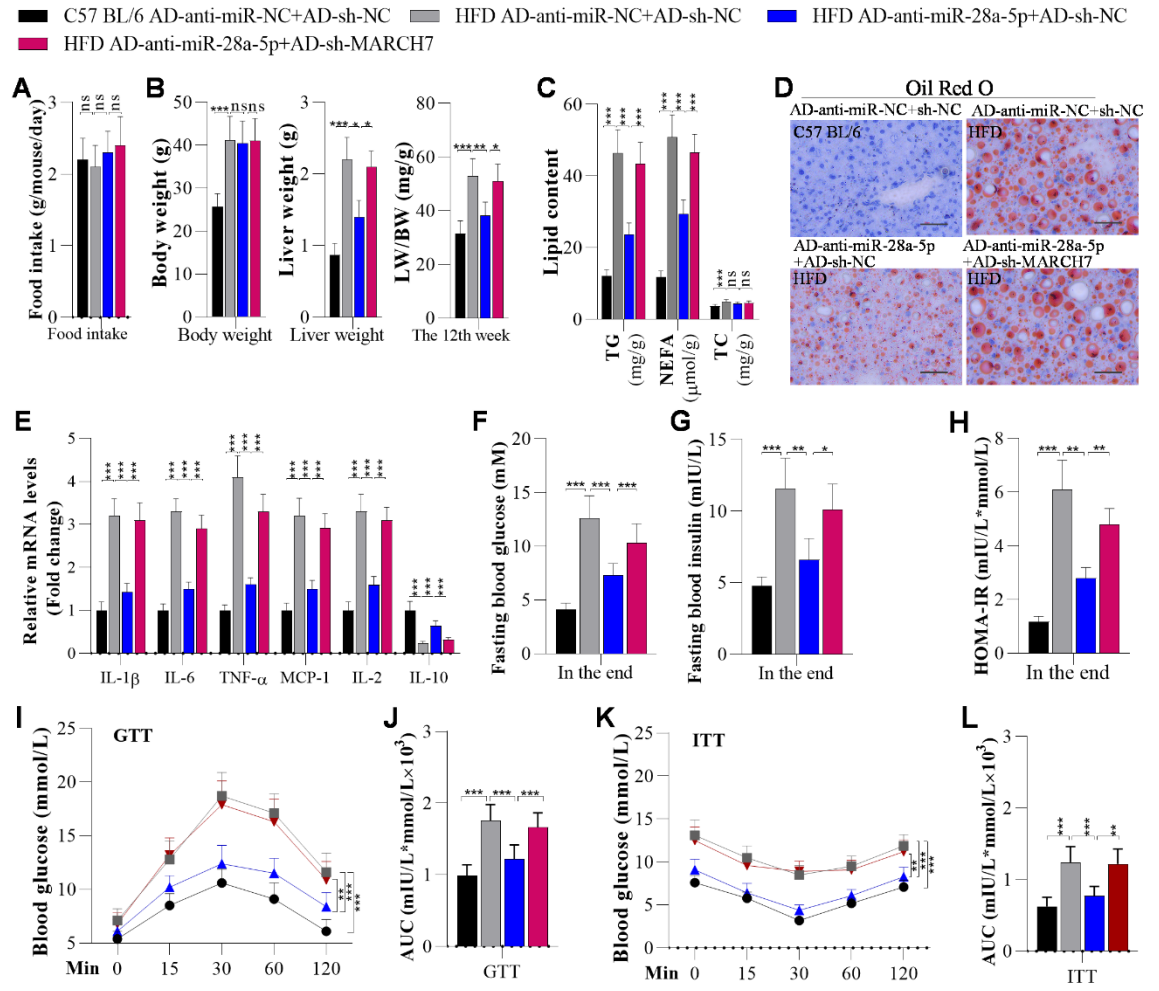

Fig. S9. **Knockdown of MARCH7 reverses anti-miR-28a-5p-mediated suppression of hepatic steatosis, inflammation, and insulin resistance in HFD-fed mice.** Mice were fed a ND or HFD for 12 weeks. Then, they were injected *once a week* with the adenoviruses AD-anti-miR-28a-5p, AD-sh-NC, AD-anti-miR-28a-5p, and AD-anti-sh-MARCH7*, and* these mice were continuously fed a ND or HFD. After 3 weeks of the first injection, the mice were used for further experiments. (**A**) The food intake of ND- and HFD-mice (n=5/group). (**B**) The body weights, liver weights, and LW/BW ratios of C57BL/6 and HFD-fed mice (n=5/group). (**C**) TG, NEFA, and TC levels were measured using ELISA in the livers of C57BL/6 and HFD-fed mice (n=5/group). (**D**) Oil Red O staining of mouse liver sections (n=5/group); Scale bar, 50 μM. (**E**) The mRNA levels of inflammation-related genes were measured by RT–qPCR (n=5/group). (**F**) Fasting blood glucose levels of C57BL/6 and HFD-fed mice (n=5/group). (**G**, **H**) Fasting insulin levels and HOMA-IR scores of adenovirus-injected C57BL/6 and HFD-fed mice (n=5/group). (**I-L**) GTT and ITT of C57BL/6 and HFD-fed mice after 3 weeks of the first adenovirus injection and the areas under the curve (AUCs) for the

GTT and ITT (N=5/group). The data are presented as the mean ± S.D. of three independent experiments. A p value of < 0.05 was considered statistically significant; and $^{*}p<0.05$, $^{**}p<0.01$, $^{***}p<0.001$ assessed via a ANOVA with the Bonferroni post hoc test for comparisons among more than two groups (A-L); ns: not significant.

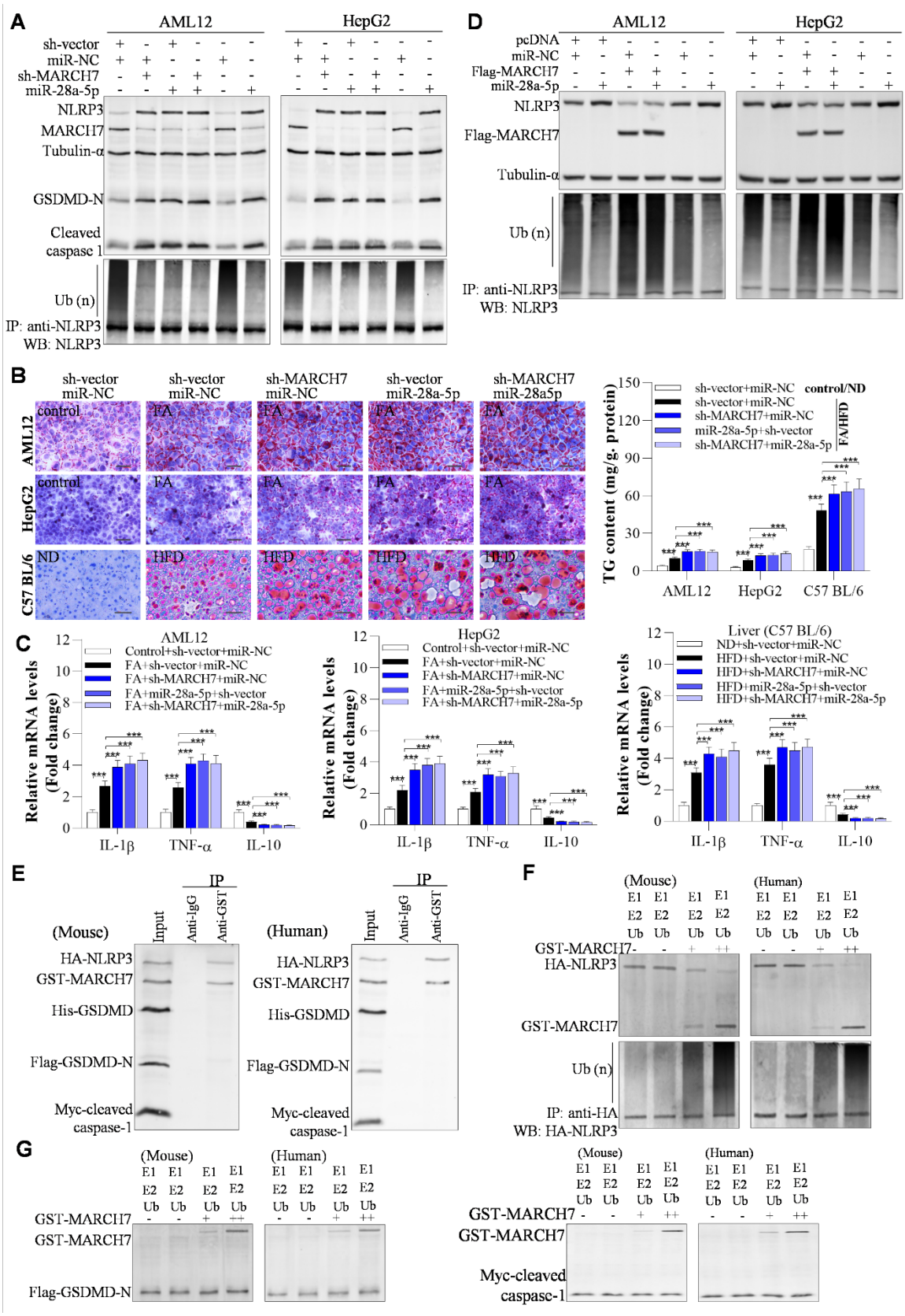

Fig. S10. MARCH7 was required for miR-28a-5p-induced inhibition of NLRP3 ubiquitination-

mediated degradation to promote pyroptosis. (**A**) After MARCH7 knockdown for 48 h, we overexpressed miR-28a-5p in AML12 and HepG2 cells for another 48 h. Then, we harvested them for Western blot analysis of pyroptosis and for analysis of NLRP3 ubiquitination after 12 h of incubation with 20 μM MG132. (**B, C**) After MARCH7 knockdown for 48 h, we overexpressed miR-28a-5p in AML12 and HepG2 cells for another 48 h, and they were incubated with FAs for 8 h; Scale bar, 50 μM. In addition, mice were fed a ND or HFD for 8 weeks. Then, they were injected with adenoviruses *every 10 days, and* these mice were continuously fed a ND or HFD. After the first injection for 3 weeks, the mice were used for Oil Red O staining, TG measurement, and RT–qPCR. (**D**) After MARCH7 overexpression for 48 h, we overexpressed miR-28a-5p in AML12 and HepG2 cells for another 48 h, and we collected them for analysis of NLRP3 ubiquitination after 12 h of incubation with 20 μM MG132. (**E**) The purified proteins were prepared by Sangon (Shanghai) and mixed together in cell lysis buffer, and the MARCH7-bound proteins were identified using a GST pull-down assay. (**F, G**) The purified proteins were mixed together in cell lysis buffer following the instructions of an *in vitro* ubiquitination assay kit (VIVA Bioscience, Amyjet Scientific Inc, Wuhan, China) and an *in vitro* ubiquitination assay protocol (DOI: 10.21769/BioProtoc.928); the effects of GST-MARCH7 on the levels of HA-NLRP3, Flag-GSDMD-N, and Myc-caspase-1 were examined by western blotting; and the ubiquitination of HA-NLRP3 was analysed. The data are presented as the mean ± S.D. of three independent experiments. A p value of < 0.05 was considered statistically significant; and $^{*}p<0.05$, $^{**}p<0.01$, $^{***}p<0.001$ assessed via a ANOVA with the Bonferroni post hoc test for comparisons among more than two groups (B, C); ns: not significant.

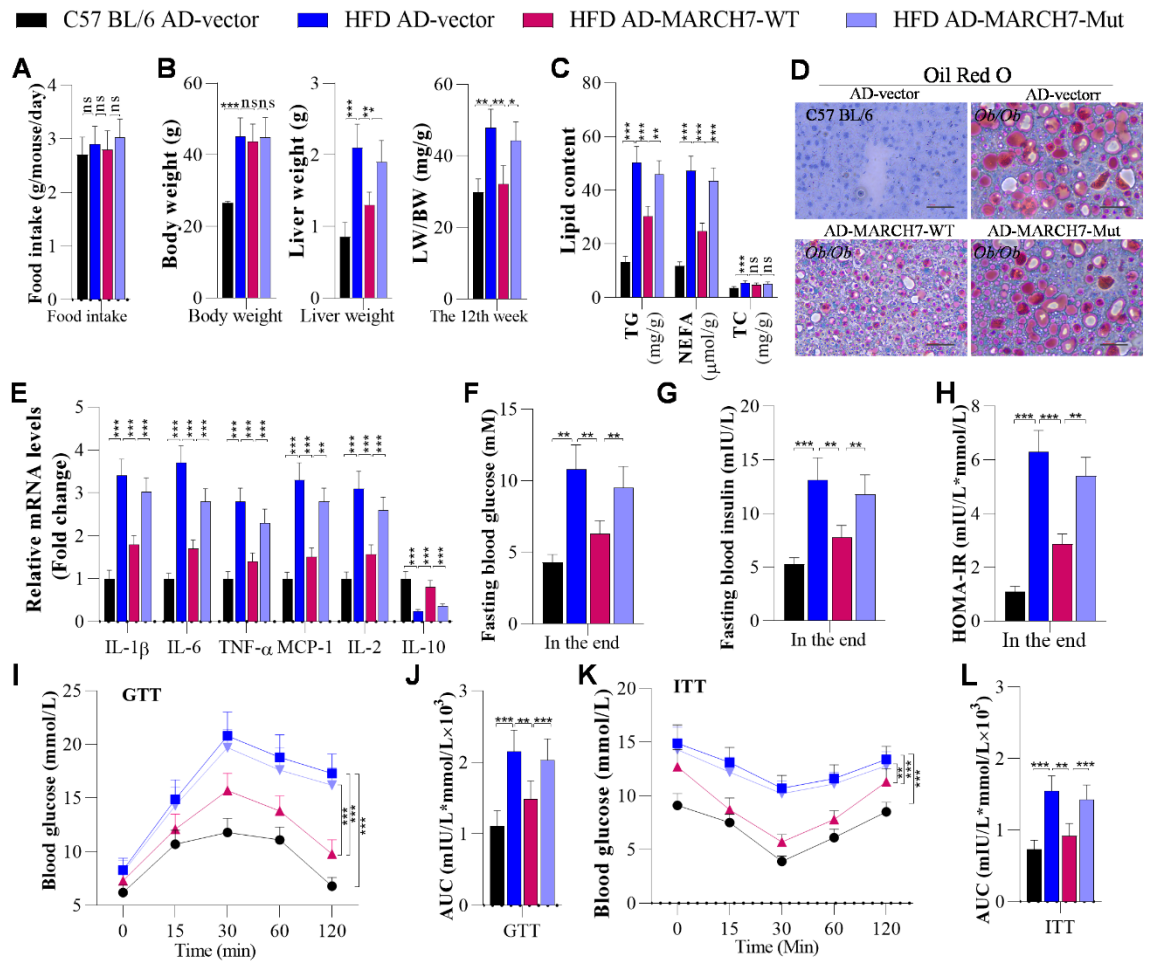

Fig. S11. **The MARCH7 mutant fails to suppress hepatic steatosis, inflammation, and insulin resistance in HFD-fed mice.** Mice were fed a ND or HFD for 12 weeks. Then, they were injected every 10 days with the adenoviruses AD-vector, AD-MARCH7-WT, and AD-MARCH7-Mut, *and* these mice were continuously fed a ND or HFD. After 3 weeks of the first injection, the mice were used for analysis. (**A**) The food intake of ND- and HFD-mice (n=5/group). (**B**) The body weights, liver weights, and LW/BW ratios of C57BL/6 and HFD-fed mice (n=5/group). (**C**) Hepatic TG, NEFA, and TC levels were measured using ELISA (n=5/group). (**D**) Oil Red O staining of mouse liver sections (n=5/group); Scale bar, 50 μM. (**E**) The mRNA levels of inflammation-related genes analysed by RT–qPCR (n=5/group). (**F**) Fasting blood glucose levels of C57BL/6 and HFD-fed mice (n=5/group). (**G**, **H**) Fasting insulin levels and HOMA-IR scores of C57BL/6 and HFD-fed mice (n=5/group). (**I-L**) GTT and ITT of C57BL/6 and HFD-fed mice and the areas under the curve (AUCs) for the GTT and ITT (N=5/group). The data are presented as the mean ± S.D. of three independent experiments. A p value of < 0.05 was considered statistically significant; and $^{*}p<0.05$, $^{**}p<0.01$, $^{***}p<0.001$ assessed via a ANOVA with the Bonferroni post hoc test for comparisons among more than two groups (A-L); ns: not significant.

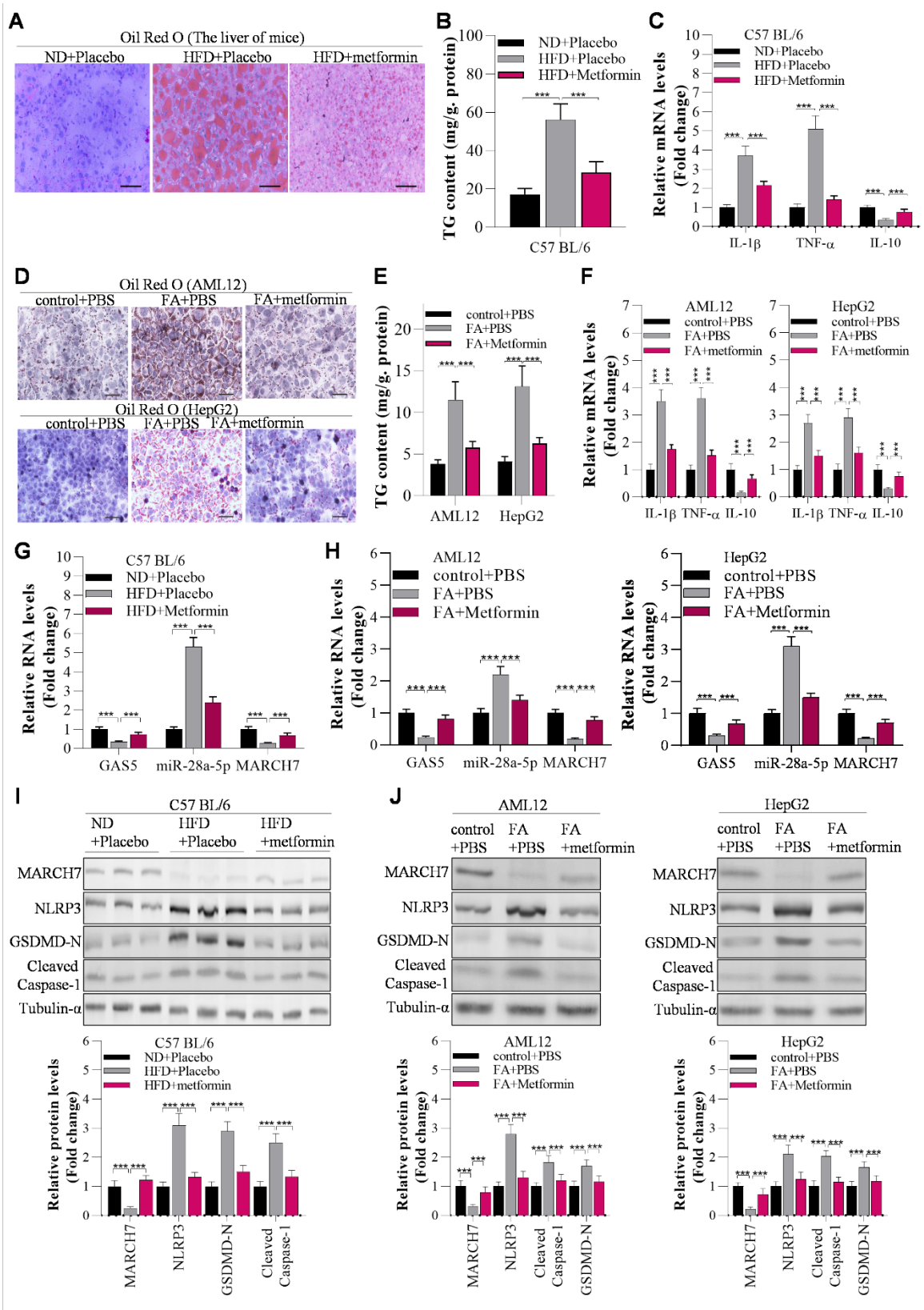

185

186 **Fig. S12. Metformin exerts anti-NAFLD activity by affecting the levels of GAS5, miR-28a-5p,**

MARCH7, and NLRP3. C57BL/6 mice (N=5) were administered daily with 200 mg metformin per kilogram of body weight for a month accompanied by 12 weeks of ND or HFD feeding. AML12 and HepG2 cells were incubated with FAs for 6 h, and they were incubated with both 10 nM metformin and FA for another 6 h. (**A**) Oil Red O staining of mouse liver sections; Scale bar, 50 μM. (**B**) The TG content was measured using ELISA in the livers of 12-week-old ND- or HFD-fed C57BL/6 mice (n=8/group). (**C**) RT–qPCR analysis of inflammatory factors in the livers of mice. (**D**) Oil Red O staining of hepatocytes (AML12 and HepG2); Scale bar, 50 μM. (**E**) The TG content was measured using ELISA in hepatocytes. (**F**) RT–qPCR analysis of inflammatory genes in hepatocytes. (**G**) RT–qPCR analysis of the expression of miR-28a-5p, MARCH7, and GAS5 in the livers of mice. (**H**) RT–qPCR analysis of the expression of miR-28a-5p, MARCH7, and GAS5 in hepatocytes. (**I**) Western blot analysis of MARCH7-mediated pyroptosis genes in the livers of mice. (**J**) Western blot analysis of MARCH7-mediated pyroptosis genes in hepatocytes. The data are presented as the mean ± S.D. of three independent experiments. The one-way analysis of variance (ANOVA) with the Bonferroni post hoc test was conducted for comparisons among more than two groups (B, C, E-J). A p value of < 0.05 was considered statistically significant; and $^{*}p < 0.05$, $^{**}p < 0.01$, $^{***}p < 0.001$; $^{ns}p > 0.05$, ns: not significant.

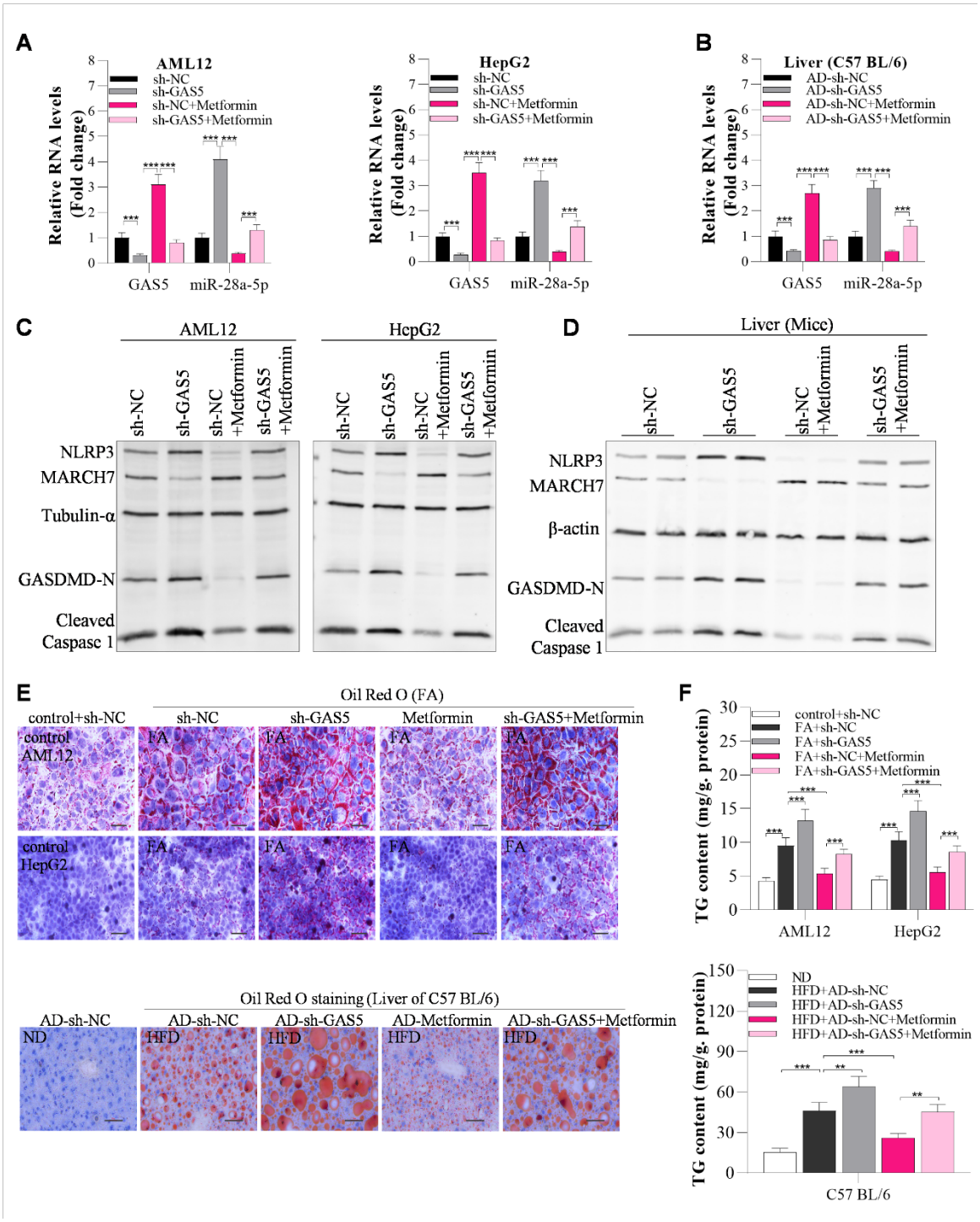

Fig. S13. Knockdown of GAS5 significantly inhibited the effects of metformin on pyroptosis and hepatic lipid deposition. After 48 h of transfection, AML12 and HepG2 cells were incubated with 10 nM metformin for another 6 h. After one week of injection of AD-GAS5, C57BL/6 mice were administered 200 mg metformin per kilogram of body weight daily for one month. Then, AML12 cells, HepG2 cells, and mouse livers were collected for further experiments. (**A**, **B**) RT–qPCR was used to determine the effects of metformin on miR-28a-5p levels in GAS5-knockdown AML12 cells, HepG2 cells, and mouse livers. (**C**, **D**)

Western blot analysis of the effects of metformin on pyroptosis in GAS5-knockdown AML12 cells, HepG2 cells, and mouse livers. (**E**, **F**) Oil Red O staining was used to examine the effects of metformin on lipid accumulation in GAS5-knockdown AML12 cells, HepG2 cells, and mouse livers; Scale bar, 50 μM. The data are presented as the mean ± S.D. of three independent experiments. The one-way analysis of variance (ANOVA) with the Bonferroni post hoc test was conducted for comparisons among more than two groups (A, B, F). A p value of < 0.05 was considered statistically significant; and $^{*}p < 0.05$, $^{**}p < 0.01$, $^{***}p < 0.001$; $^{ns}p > 0.05$, ns: not significant.